

Amide Proton Transfer Magnetic Resonance Imaging of Alzheimer's Disease at 3.0 Tesla: A Preliminary Study

Rui Wang¹, Sa-Ying Li¹, Min Chen¹, Jin-Yuan Zhou², Dan-Tao Peng³, Chen Zhang¹, Yong-Ming Dai⁴

¹Department of Radiology, Beijing Hospital, Beijing 100730, China

²Department of Radiology, Division of MR Research, Johns Hopkins University, Baltimore, Maryland 21287, USA

³Department of Neurology, China-Japan Friendship Hospital, Beijing 100029, China

⁴Imaging System, Philips Healthcare, MR, Shanghai 200233, China

Abstract

Background: Amide proton transfer (APT) imaging has recently emerged as an important contrast mechanism for magnetic resonance imaging (MRI) in the field of molecular and cellular imaging. The aim of this study was to evaluate the feasibility of APT imaging to detect cerebral abnormality in patients with Alzheimer's disease (AD) at 3.0 Tesla.

Methods: Twenty AD patients (9 men and 11 women; age range, 67–83 years) and 20 age-matched normal controls (11 men and 9 women; age range, 63–82 years) underwent APT and traditional MRI examination on a 3.0 Tesla MRI system. The magnetic resonance ratio asymmetry (MTR_{asym}) values at 3.5 ppm of bilateral hippocampi (Hc), temporal white matter regions, occipital white matter regions, and cerebral peduncles were measured on oblique axial APT images. MTR_{asym} (3.5 ppm) values of the cerebral structures between AD patients and control subjects were compared with independent samples *t*-test. Controlling for age, partial correlation analysis was used to investigate the associations between mini-mental state examination (MMSE) and the various MRI measures among AD patients.

Results: Compared with normal controls, MTR_{asym} (3.5 ppm) values of bilateral Hc were significantly increased in AD patients (right $1.24\% \pm 0.21\%$ vs. $0.83\% \pm 0.19\%$, left $1.18\% \pm 0.18\%$ vs. $0.80\% \pm 0.17\%$, $t = 3.039, 3.328, P = 0.004, 0.002$, respectively). MTR_{asym} (3.5 ppm) values of bilateral Hc were significantly negatively correlated with MMSE (right $r = -0.559, P = 0.013$; left $r = -0.461, P = 0.047$).

Conclusions: Increased MTR_{asym} (3.5 ppm) values of bilateral Hc in AD patients and its strong correlations with MMSE suggest that APT imaging could potentially provide imaging biomarkers for the noninvasive molecular diagnosis of AD.

Key words: Alzheimer's Disease; Amide Proton Transfer Imaging; Molecular Imaging

INTRODUCTION

Alzheimer's disease (AD), one of the progressive neurodegenerative diseases, is known as the leading cause of dementia in the elderly.^[1] Imaging biomarkers from a variety of magnetic resonance (MR) techniques for risk and disease progression are crucial to understand and monitor the disease.^[2-6] Initially, volume measurements of the hippocampus (Hc) and other medial temporal structures were used to differentiate AD from healthy subjects.^[2,7] However, an overlap was found between patients and control groups.^[7] Moreover, most patients with cerebral atrophy detected on MR imaging (MRI) often have irreversible pathological damage to the brain. The use of advanced MRI techniques, such as arterial spin labeling imaging,^[3] susceptibility-weighted imaging,^[6] and

magnetization transfer imaging,^[2] may increase the accuracy of AD diagnosis. Nevertheless, these methods are not very satisfying in terms of the diagnosis of AD to date. A further reliable imaging technique for AD is still desired.

Amide proton transfer (APT) imaging is a novel molecular MRI technique that detects low-concentration endogenous mobile proteins and peptides in tissue noninvasively. It can indirectly reflect intracellular metabolic change and physiological and pathological information *in vivo*.^[8-10] Most current studies about APT focus on tumors and stroke.^[8-10] APT imaging is able to detect tissue pH changes in stroke (where pH decreases),^[8] and identify the spatial extent and pathological grade of some tumors due to increased mobile protein and peptide.^[9,10] Recently, molecular pathology studies have shown that most neurodegenerative diseases, including AD, are associated with accumulations of abnormal proteins in the central nervous system.^[11] So far, no study has been published about using APT imaging on AD patients, and whether APT imaging can provide unique information about AD is still unknown.

Access this article online

Quick Response Code:



Website:
www.cmj.org

DOI:
10.4103/0366-6999.151658

Address for correspondence: Dr. Min Chen,
Department of Radiology, Beijing Hospital, Beijing 100730, China
E-Mail: chenmin62@yahoo.com

This study aimed to test the feasibility of using APT imaging to detect cerebral abnormality in patients with AD at field strength of 3 Tesla. The pathological findings of AD include the accumulation of amyloid plaques, neurofibrillary tangles, and neuronal loss.^[1,2] And AD neuropathology is thought to begin in the medial temporal lobe, particularly the Hc, and then spreads throughout neocortex, so the Hc is affected very early and severely in AD.^[12,13] Except for these cortical structures, the white matter is also damaged.^[4,14] Thus, we hypothesize that the accumulations of abnormal cytoplasmic proteins in some specific cerebral areas (such as Hc) is associated with high APT signal.

METHODS

Subjects

Twenty-five AD patients and 21 age-matched healthy elderly subjects were enrolled in the study (however, 2 severe AD patients did not finished MRI scans because of restlessness, and 3 AD patients and 1 healthy control were excluded because of motion artifacts on APT images. Hence, the data of only 20 AD patients and 20 healthy controls were analyzed statistically). AD patients were recruited from a Memory Clinic at the Department of Neurology from May, 2013 to February, 2014. Healthy elderly subjects were recruited from nearby communities. The diagnosis of AD was made according to the criteria of the National Institute of Neurological and Communicative Disorders and Stroke/AD and Related Disorders Association.^[15] The mini-mental state examination (MMSE) was performed on all subjects. Based on the criteria of the Diagnostic and Statistical Manual of Mental Disorders, Fourth Edition,^[16] 10 patients with AD had mild disease severity, 6 had moderate, and 4 had severe. Healthy control subjects had no subjective complaints of memory or other cognitive impairment and had no major neurologic, psychiatric, or systemic illness that might affect cognitive function. The demographics and neuropsychological findings of AD patients and healthy elderly subjects are shown in Table 1.

This study was approved by the local Institutional Review Board. Written informed consents were signed by all subjects prior to the study.

Magnetic resonance imaging data acquisition

The MR examinations were performed on a 3.0 T MRI system (Achieva TX, Philips Healthcare, Best, The Netherlands), using an eight-channel head coil. Pencil beam second-

order shimming was employed. Prior to APT imaging, three-dimensional (3D) volumetric sagittal T1-weighted images covering the whole brain and coronal fluid-attenuated inversion recovery (FLAIR) images perpendicular to the long axis of the Hc, were obtained to better observe medial temporal structures.

Amide proton transfer imaging was based on a single-shot, turbo-spin-echo readout, with the following parameters: repetition time 3000 ms, turbo-spin-echo factor 54, field of view 230 mm × 220 mm, matrix 105 × 100; slice thickness 5 mm. The axial scanning plane is parallel to the long axis of the Hc.^[17] We used a pseudo-continuous wave, off-resonance radio frequency (RF) irradiation (saturation duration 200 ms × 4, inter-pulse delay 10 ms, power level 2 μT) and a multi-offset, multi-acquisition APT imaging protocol.^[18] The 31 offsets were 0, ±0.25, ±0.5, ±0.75, ±1 (2), ±1.5 (2), ±2 (2), ±2.5 (2), ±3 (2), ±3.25 (2), ±3.5 (8), ±3.75 (2), ±4 (2), ±4.5, ±5, ±6 ppm (the values in parentheses represented the number of acquisitions, which was one, if not specified). An unsaturated image was obtained for the signal normalization. The acquisition time was 2 min 40 s.

Data processing

The APT imaging analysis was performed using in-house developed software, based on the Interactive Data Language (IDL, ITT Visual Information Solutions, Boulder, CO, USA) environment. The composite backbone amide resonance of endogenous mobile proteins is around 8.3 ppm in the proton nuclear MR spectrum (which is 3.5 ppm downfield from water). The APT effects were quantified according to the following equation:

$$\begin{aligned} \text{MTR}_{\text{asym}}(3.5 \text{ ppm}) &= \text{MTR}(+3.5 \text{ ppm}) - \text{MTR}(-3.5 \text{ ppm}) \\ &= S_{\text{sat}}(-3.5 \text{ ppm})/S_0 - S_{\text{sat}}(+3.5 \text{ ppm})/S_0^{[18]} \end{aligned}$$

Note: Magnetic resonance ratio asymmetry (MTR_{asym}) (3.5 ppm) is the abbreviation of magnetization transfer ratio asymmetry at 3.5 ppm. S_{sat} and S_0 represent the signal intensities with and without selective RF irradiation, respectively.

To correct for the B_0 field inhomogeneity effect, as described previously,^[18] the raw image data were first organized into the z-spectrum (the normalized signal intensities, S_{sat}/S_0 , as a function of 31 offsets). Then, the z-spectrum was fitted through all offsets using a 12th-order polynomial (the maximum order available with IDL) on a voxel-by-voxel basis. The fitted curve was interpolated using an offset resolution of 1 Hz. After this step, the corresponding B_0 field inhomogeneity was calculated according to the deviation of the minimum of the fitted curve from 0 ppm. To correct the field inhomogeneity effect, the original z-spectrum was interpolated and centered along the direction of the offset axis to shift its lowest intensity to 0 ppm. The realigned z-spectra were interpolated back to 31 points. Finally, the APT-weighted image (namely, $\text{MTR}_{\text{asym}}[3.5 \text{ ppm}]$ image) was calculated using the B_0 -corrected data at the offset of ±3.5 ppm. The image was thresholded based on the signal intensity of S_0 image to remove voxels outside the brain.

Table 1: Demographics and neuropsychological findings of normal subjects and AD patients

Groups	Normal subjects	AD patients	t	P
Age (years)	71.9 ± 5.0	73.7 ± 4.7	1.175	0.247
Male/female (n/n)	11/9	9/11	0.400*	0.527
MMSE scores	28.6 ± 1.0	16.9 ± 7.0	-7.283	0.000

*Two-sample t-test for all comparisons except sex, where Pearson χ^2 -test was used. MMSE: Mini-mental state examination; AD: Alzheimer's disease.

The quantitative image analysis of APT was performed. The T1-weighted image was used as the anatomical reference to draw regions of interest (ROIs) of bilateral Hc, temporal white matter (TWM), occipital white matter (OWM) and cerebral peduncles (CPs) were measured on the oblique axial APT image, as shown in Figure 1. The ROIs were drawn to include as much of the measured tissues as possible while avoiding the adjacent cerebrospinal fluid (CSF) containing spaces to decrease partial volume effects from fluid. MTR_{asym} (3.5 ppm) were measured for each region. Each Hc was manually traced to include the head, body, and tail of the Hc as described previously.^[17,19] The CP was chosen as a control region, in the vicinity of Hc but not typically affected in AD. Although AD is predominantly a gray matter disease, ROIs of bilateral TWM and OWM were outlined as white matter was also mildly damaged.^[2,4,14]

Statistical analysis

All data were analyzed using the statistical package SPSS (Version 16, Chicago, IL). Demographic, MMSE, and imaging data of AD patients and control subjects were compared using the independent samples *t*-test, except for sex, where Pearson χ^2 -test was used. The average MTR_{asym} (3.5 ppm) and corresponding 95% confidence intervals were calculated for each region. Controlling for age, partial correlation analysis was used to investigate the associations between MMSE and the various MRI measures among patients with AD. The level of significance was set at $P < 0.05$.

RESULTS

Subjects

AD patients and control subjects were not significantly different in terms of age and sex. AD patients had significantly lower mean MMSE than control subjects [Table 1].

Amide proton transfer results

Two examples of the FLAIR images and APT-weighted images for a normal control and an AD patient were shown in Figure 2. Compared with the normal subject, we found marked atrophy and elevated APT-weighted intensities in both of the Hc in the AD patient.

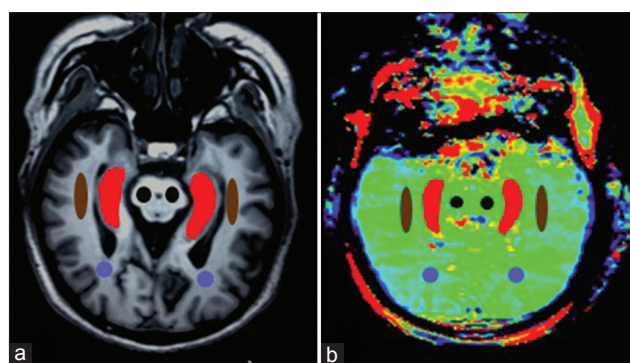


Figure 1: T1-weighted image (a) and amide proton transfer image (b) were oblique axial planes along the long axis the hippocampi (Hc). Examples of the definition of the regions of interest for quantitative analysis (Brown: Temporal white matter; Purple: Occipital white matter; Black: Cerebral peduncle; Red: Hc).

Table 2 compared MTR_{asym} (3.5 ppm) values of bilateral Hc, TWM, OWM, and CP in normal controls and AD patients. We found that MTR_{asym} (3.5 ppm) values of bilateral Hc were significantly higher in AD patients than in normal controls. The additions are equivalent to approximately 49% for the right Hc and 47% for the left Hc, respectively. However, no significant differences in MTR_{asym} (3.5 ppm) values of other brain structures were observed between AD patients and normal controls.

Associations between amide proton transfer measures and mini-mental state examination

Table 3 shows that the correlation coefficients for the relationships between MMSE scores and MTR_{asym} (3.5 ppm) values of cerebral structures among AD patients. Partial

Table 2: MTR_{asym} (3.5 ppm) values (mean \pm 95% CI) of bilateral Hc, TWM, OWM, and CP in normal controls and AD patients

	Control subjects (n = 20)	Patients with AD (n = 20)	t	P
Right Hc	0.83 \pm 0.19	1.24 \pm 0.21	3.039	0.004*
Left Hc	0.80 \pm 0.17	1.18 \pm 0.18	3.238	0.002*
Right TWM	0.39 \pm 0.08	0.42 \pm 0.09	0.636	0.529
Left TWM	0.34 \pm 0.06	0.38 \pm 0.10	0.699	0.489
Right OWM	0.32 \pm 0.07	0.36 \pm 0.12	0.591	0.558
Left OWM	0.38 \pm 0.09	0.34 \pm 0.09	0.604	0.549
Right CP	1.03 \pm 0.15	1.14 \pm 0.22	0.778	0.442
Left CP	1.09 \pm 0.19	1.19 \pm 0.21	0.703	0.487

*Significant change. CI: Confidence interval; AD: Alzheimer's disease; CP: Cerebral peduncles; OWM: Occipital white matter; TWM: Temporal white matter; Hc: Hippocampus; MTR_{asym} : Magnetic resonance ratio asymmetry.

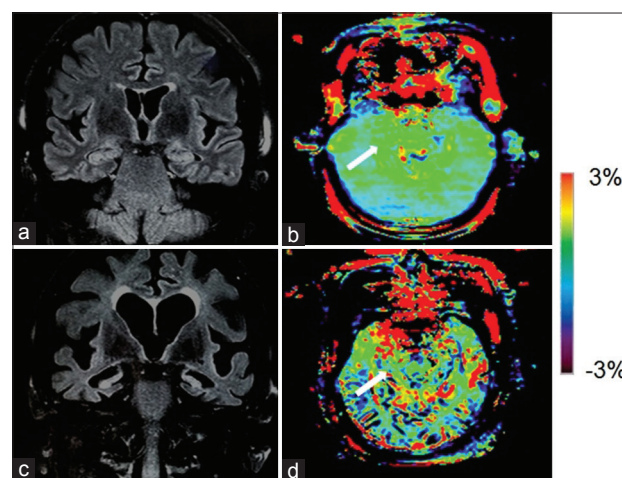


Figure 2: Fluid attenuated inversion recovery (FLAIR) image (a) and amide proton transfer (APT)-weighted image (b) of a typical normal control (female, 72 years old, mini-mental state examination [MMSE] score 29). FLAIR image (c) and APT image (d) of an Alzheimer's disease (AD) patient (female, 70 years old, MMSE score 16). Atrophy of bilateral hippocampi (Hc), enlarged lateral ventricles and widened sulci in AD were seen on the coronal FLAIR image. The APT-weighted intensities in regions of the Hc (white arrow) were higher in AD patients than in normal controls.

correlation analysis revealed only MTR_{asym} (3.5 ppm) values of bilateral Hc were significantly associated with MMSE (right $r = -0.559$, $P = 0.013$; left $r = -0.461$, $P = 0.047$). There were no correlations between MMSE and MTR_{asym} (3.5 ppm) values in bilateral TWM, OWM, and CP. Scatters [Figure 3] demonstrated MTR_{asym} (3.5 ppm) values of bilateral Hc were negatively correlated with MMSE.

DISCUSSION

Amide proton transfer is a special type of chemical exchange dependent saturation transfer (CEST) MRI that detects mobile proteins and peptides in tissue (such as those in the cytoplasm). The technique is unlike the traditional magnetization transfer imaging method that is sensitive to solid-like proteins in tissue.^[20] Its basic principle is that amide protons in the peptide bonds are saturated, and then chemical exchange happens between amide protons and free water protons.^[8,21] The exchange speed has been demonstrated to be mainly relevant to amide proton concentration and pH value in the tissue.^[22-25] The higher the concentration of the amide proton is, the faster the exchange rate is, and thus the higher the APT value is.^[8] AD is also associated with accumulations of abnormal proteins in the brain.^[11] Some of these increased abnormal proteins are intracellular and soluble, including A β oligomer, Tau, α -synuclein, TDP-43, and so on.^[26-29] Soluble oligomeric forms of A β are now believed to induce the deleterious cascade(s) involved in the pathophysiology of AD.^[26] There are three types of tau protein including insoluble hyperphosphorylated tau protein, soluble phosphorylated and nonphosphorylated tau protein in AD brain.^[27] α -synuclein is a neuronal cytoplasmic protein. In AD with Lewy bodies, an accumulation of α -synuclein containing Lewy body inclusions is the major intracellular pathology.^[28] These molecular results indicate the APT is a potential method that can noninvasively visualize the protein content of AD *in vivo*.

In this study, we found that the signal intensities of bilateral Hc were higher in AD patients than in normal controls on Figure 2. Further quantitative analysis also showed that compared to normal controls, MTR_{asym} (3.5 ppm) values of

bilateral Hc increased in AD patients. In contrast, there were no significant statistically differences in MTR_{asym} (3.5 ppm) values of other cerebral structures between AD patients and control subjects. There may be two reasons for the findings: (1) The Hc is affected the earliest and most severely in AD patients.^[12] (2) Elevated MTR_{asym} (3.5 ppm) values of the Hc in AD patients may be associated with increased cytosolic proteins and peptides.^[26-28]

Based on Table 3 and Figure 3, we observed that MTR_{asym} (3.5 ppm) values of only bilateral Hc were negatively correlated with MMSE. The results indicated that hippocampal MTR_{asym} (3.5 ppm) values could not only distinguish AD patients from controls, but also correlate well with the disease severity of AD. This will help to monitor the condition of patients with AD.

This study had several limitations. One limitation was that one scan can only obtain single-slice images due to the limitation of acquisition protocol. Thus, the MRI signal changes in other regions could not be evaluated in the present study. A new highly sensitive 3D whole-brain pulsed steady-state CEST technology has been reported recently.^[30] A second limitation was that it was a little difficult to draw ROIs of cerebral structures exactly due to the limited

Table 3: Partial correlation coefficients (r) for the associations between MMSE and the various MRI measures among patients with AD

	r	P
Right Hc	-0.559	0.013*
Left Hc	-0.461	0.047*
Right TWM	-0.102	0.679
Left TWM	-0.296	0.219
Right OWM	0.175	0.475
Left OWM	0.279	0.247
Right CP	0.196	0.420
Left CP	0.128	0.602

*The difference was significant statistically. AD: Alzheimer's disease; CP: Cerebral peduncles; OWM: Occipital white matter; TWM: Temporal white matter; Hc: Hippocampus; MRI: Magnetic resonance imaging; MMSE: Mini-mental state examination.

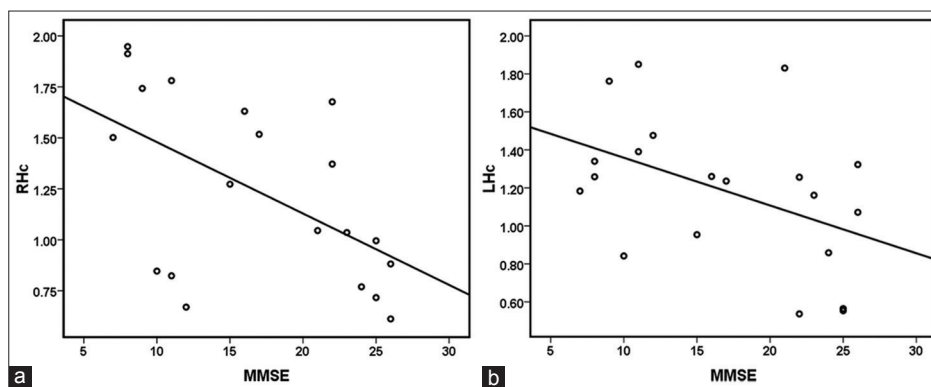


Figure 3: Scatter of correlation between mini-mental state examination (MMSE) and magnetic resonance ratio asymmetry (MTR_{asym}) (3.5 ppm) in right hippocampi (Hc) (a) and Scatter of correlation between MMSE and MTR_{asym} (3.5 ppm) in left Hc (b). MTR_{asym} (3.5 ppm) values of bilateral Hc both showed a negative correlation with MMSE.

resolution of APT imaging. Meanwhile, the measurement of the Hc may be affected by the surrounding CSF. This may have influenced the accuracy of our results to some extent.

In conclusion, as a safe, completely noninvasive MR technology, the APT imaging is able to generate image contrasts based on the changes in cytoplasmic proteins and peptides in specific brain regions in AD patients. Meanwhile, the hippocampal MTR_{asym} (3.5 ppm) values have strong correlations with MMSE scores in AD patients. The results suggest APT is a useful tool to diagnose AD and monitor the disease progression.

REFERENCES

1. Xi Q, Zhao XH, Wang PJ, Guo QH, Yan CG, He Y. Functional MRI study of mild Alzheimer's disease using amplitude of low frequency fluctuation analysis. *Chin Med J* 2012;125:858-62.
2. Ridha BH, Symms MR, Tozer DJ, Stockton KC, Frost C, Siddique MM, *et al.* Magnetization transfer ratio in Alzheimer disease: Comparison with volumetric measurements. *AJNR Am J Neuroradiol* 2007;28:965-70.
3. Johnson NA, Jahng GH, Weiner MW, Miller BL, Chui HC, Jagust WJ, *et al.* Pattern of cerebral hypoperfusion in Alzheimer disease and mild cognitive impairment measured with arterial spin-labeling MR imaging: Initial experience. *Radiology* 2005;234:851-9.
4. Racine AM, Adluru N, Alexander AL, Christian BT, Okonkwo OC, Oh J, *et al.* Associations between white matter microstructure and amyloid burden in preclinical Alzheimer's disease: A multimodal imaging investigation. *Neuroimage Clin* 2014;4:604-14.
5. Takahashi H, Ishii K, Hosokawa C, Hyodo T, Kashiwagi N, Matsuki M, *et al.* Clinical application of 3D arterial spin-labeled brain perfusion imaging for Alzheimer disease: Comparison with brain perfusion SPECT. *AJNR Am J Neuroradiol* 2014;35:906-11.
6. Yates PA, Sirisriro R, Villemagne VL, Farquharson S, Masters CL, Rowe CC, *et al.* Cerebral microhemorrhage and brain β -amyloid in aging and Alzheimer disease. *Neurology* 2011;77:48-54.
7. Clerx L, van Rossum IA, Burns L, Knol DL, Scheltens P, Verhey F, *et al.* Measurements of medial temporal lobe atrophy for prediction of Alzheimer's disease in subjects with mild cognitive impairment. *Neurobiol Aging* 2013;34:2003-13.
8. Zhou J, Payen JF, Wilson DA, Traystman RJ, van Zijl PC. Using the amide proton signals of intracellular proteins and peptides to detect pH effects in MRI. *Nat Med* 2003;9:1085-90.
9. Zhou J, Tryggestad E, Wen Z, Lal B, Zhou T, Grossman R, *et al.* Differentiation between glioma and radiation necrosis using molecular magnetic resonance imaging of endogenous proteins and peptides. *Nat Med* 2011;17:130-4.
10. Zhou J, Hong X, Zhao X, Gao JH, Yuan J. APT-weighted and NOE-weighted image contrasts in glioma with different RF saturation powers based on magnetization transfer ratio asymmetry analyses. *Magn Reson Med* 2013;70:320-7.
11. Peden AH, Ironside JW. Molecular pathology in neurodegenerative diseases. *Curr Drug Targets* 2012;13:1548-59.
12. Du AT, Schuff N, Amend D, Laakso MP, Hsu YY, Jagust WJ, *et al.* Magnetic resonance imaging of the entorhinal cortex and hippocampus in mild cognitive impairment and Alzheimer's disease. *J Neurol Neurosurg Psychiatry* 2001;71:441-7.
13. Ezekiel F, Chao L, Kornak J, Du AT, Cardenas V, Truran D, *et al.* Comparisons between global and focal brain atrophy rates in normal aging and Alzheimer disease: Boundary Shift Integral versus tracing of the entorhinal cortex and hippocampus. *Alzheimer Dis Assoc Disord* 2004;18:196-201.
14. Capizzano AA, Ación L, Bekinschtein T, Furman M, Gomila H, Martínez A, *et al.* White matter hyperintensities are significantly associated with cortical atrophy in Alzheimer's disease. *J Neurol Neurosurg Psychiatry* 2004;75:822-7.
15. McKhann G, Drachman D, Folstein M, Katzman R, Price D, Stadlan EM. Clinical diagnosis of Alzheimer's disease: Report of the NINCDS-ADRDA Work Group under the auspices of Department of Health and Human Services Task Force on Alzheimer's Disease. *Neurology* 1984;34:939-44.
16. Chapman RM, Mapstone M, McCrary JW, Gardner MN, Porsteinsson A, Sandoval TC, *et al.* Predicting conversion from mild cognitive impairment to Alzheimer's disease using neuropsychological tests and multivariate methods. *J Clin Exp Neuropsychol* 2011;33:187-99.
17. Londoño A, Castillo M, Lee YZ, Smith JK. Apparent diffusion coefficient measurements in the hippocampi in patients with temporal lobe seizures. *AJNR Am J Neuroradiol* 2003;24:1582-6.
18. Wen Z, Hu S, Huang F, Wang X, Guo L, Quan X, *et al.* MR imaging of high-grade brain tumors using endogenous protein and peptide-based contrast. *Neuroimage* 2010;51:616-22.
19. Beaurain J, Dormont D, Semah F, Hasboun D, Baulac M. Hippocampal formations imaging with axial sections parallel to their longitudinal axis. *Magn Reson Imaging* 1994;12:139-48.
20. Henkelman RM, Stanisz GJ, Graham SJ. Magnetization transfer in MRI: A review. *NMR Biomed* 2001;14:57-64.
21. Jokivarsi KT, Gröhn HI, Gröhn OH, Kauppinen RA. Proton transfer ratio, lactate, and intracellular pH in acute cerebral ischemia. *Magn Reson Med* 2007;57:647-53.
22. Dula AN, Arlinghaus LR, Dortch RD, Dewey BE, Whisenant JG, Ayers GD, *et al.* Amide proton transfer imaging of the breast at 3 T: Establishing reproducibility and possible feasibility assessing chemotherapy response. *Magn Reson Med* 2013;70:216-24.
23. Zhou J, Zhu H, Lim M, Blair L, Quinones-Hinojosa A, Messina SA, *et al.* Three-dimensional amide proton transfer MR imaging of gliomas: Initial experience and comparison with gadolinium enhancement. *J Magn Reson Imaging* 2013;38:1119-28.
24. Zhao X, Wen Z, Huang F, Lu S, Wang X, Hu S, *et al.* Saturation power dependence of amide proton transfer image contrasts in human brain tumors and strokes at 3 T. *Magn Reson Med* 2011;66:1033-41.
25. Sun PZ, Zhou J, Sun W, Huang J, van Zijl PC. Detection of the ischemic penumbra using pH-weighted MRI. *J Cereb Blood Flow Metab* 2007;27:1129-36.
26. Larson ME, Lesné SE. Soluble A β oligomer production and toxicity. *J Neurochem* 2012;120 Suppl 1:125-39.
27. Köpke E, Tung YC, Shaikh S, Alonso AC, Iqbal K, Grundke-Iqbal I. Microtubule-associated protein tau. Abnormal phosphorylation of a non-paired helical filament pool in Alzheimer disease. *J Biol Chem* 1993;268:24374-84.
28. Xu G, Stevens SM Jr, Moore BD, McClung S, Borchelt DR. Cytosolic proteins lose solubility as amyloid deposits in a transgenic mouse model of Alzheimer-type amyloidosis. *Hum Mol Genet* 2013;22:2765-74.
29. Amador-Ortiz C, Lin WL, Ahmed Z, Personett D, Davies P, Duara R, *et al.* TDP-43 immunoreactivity in hippocampal sclerosis and Alzheimer's disease. *Ann Neurol* 2007;61:435-45.
30. Jones CK, Polders D, Hua J, Zhu H, Hoogduin HJ, Zhou J, *et al.* *In vivo* three-dimensional whole-brain pulsed steady-state chemical exchange saturation transfer at 7 T. *Magn Reson Med* 2012;67:1579-89.

Received: 23-10-2014 **Edited by:** Yi Cui

How to cite this article: Wang R, Li SY, Chen M, Zhou JY, Peng DT, Zhang C, Dai YM. Amide Proton Transfer Magnetic Resonance Imaging of Alzheimer's Disease at 3.0 Tesla: A Preliminary Study. *Chin Med J* 2015;128:615-9.

Source of Support: This work was supported by grants from the National Science and Technology Pillar Program during the 12th Five-year Plan Period of China (No. 2012BAI10B04) and the National Institutes of Health (R01NS083425, R01EB009731, and R01CA166171).

Conflict of Interest: None declared.